(fwhm) pulses. The white light (1:1 $D_2O/H_2O$) probe beam was detected by a dual diode array (Princeton Instruments DDA512) consisting of 512 elements as described elsewhere.[81] The transient spectra in Figures 7 and 8 were obtained by averaging 300-500 shots, and the system was calibrated relative to the transient spectrum of the anthracene cation radical.[82]

(81) Sankararaman, S.; Kochi, J. K. *J. Chem. Soc., Perkin Trans. 2*, in press.
(82) Compare: Mataga, N.; Shioyama, H.; Kanda, Y. *J. Phys. Chem.* **1987**, *91*, 314. See also: References 19 and 30.

**Acknowledgment.** We thank T. M. Bockman for providing critical ideas and suggestions, J. D. Korp for crystallographic assistance, Z. Karpinski for the electrochemical measurements, S. Sankararaman for the time-resolved spectra, and the National Science Foundation, Robert A. Welch Foundation, and the Texas Advanced Research Program for financial support.

**Supplementary Material Available:** Tables of the observed and calculated structure factors for $[Cp_2Fe, (DUR)_2Fe^{2+}(PF_6^-)_2]$ and [durene, $(HMB)_2Fe^{2+}(PF_6^-)_2$] (17 pages). Ordering information is given on any current masthead page.

# Factors Determining the Site of Electroreduction in Nickel Metalloporphyrins. Spectral Characterization of Ni(I) Porphyrins, Ni(II) Porphyrin $\pi$-Anion Radicals, and Ni(II) Porphyrin $\pi$-Anion Radicals with Some Ni(I) Character

**K. M. Kadish,* M. M. Franzen, B. C. Han, C. Araullo-McAdams, and D. Sazou**

*Contribution from the Department of Chemistry, University of Houson, Houston, Texas 77204-5641.* *Received July 2, 1990*

**Abstract:** The effect of temperature, porphyrin macrocycle, and solvent on the electroreduction of $(P)Ni^{II}$ where P is the dianion of *meso*-tetrakis(*p*-(diethylamino)phenyl)porphyrin ($T(p\text{-}Et_2N)PP$) or *meso*-tetrakis(*o,o,m,m*-tetrafluoro-*p*-(dimethylamino)phenyl)porphyrin ($T(p\text{-}Me_2N)F_4PP$) is reported. Both compounds were reduced by controlled potential electrolysis and characterized by ESR and UV-visible spectroscopy. The site of electron transfer varied as a function of experimental conditions and the stable electrogenerated products were assigned as Ni(I) porphyrins, Ni(II) porphyrin $\pi$-anion radicals, or Ni(II) porphyrin $\pi$-anion radicals with some Ni(I) character. Ni(I) ESR spectra were obtained for $[(T(p\text{-}Et_2N)PP)Ni]^-$ and $[(T(p\text{-}Me_2N)F_4PP)Ni]^-$ at low temperature in THF under a CO atmosphere as well as in DMF or pyridine under $N_2$. In contrast, ESR spectra of Ni(II) porphyrin $\pi$-anion radicals or Ni(II) porphyrin $\pi$-anion radicals with some Ni(I) character were obtained in THF under $N_2$ at room and low temperature, respectively. $[(T(p\text{-}Et_2N)PP)Ni]^-$ catalytically reduces $CH_3I$ at room temperature, consistent with the presence of some Ni(I) character in the reactive species. $[(T(p\text{-}Me_2N)F_4PP)Ni]^-$ also reacts with $CH_3I$, but this reaction is not catalytic at room temperature and one or more $\beta$ pyrrole methylated nickel chlorins are formed as stable products. These species were characterized by UV-visible spectroscopy, $^1H$ NMR spectroscopy, and mass spectrometry and give data which suggests a high electron density on the porphyrin macrocycle of $[(T(p\text{-}Me_2N)F_4PP)N]^-$.

## Introduction

The electroreduction of synthetic nickel(II) porphyrins,[1-9] chlorins[3,6,8] and isobacteriochlorins[6-8] proceeds via one or two one-electron transfer reactions in nonaqueous media. The product of the first reduction may be assigned as a Ni(II) porphyrin $\pi$-anion radical, a Ni(I) porphyrin anion, or a mixture of both as shown in Scheme I where L is the dianion of a given porphyrin, chlorin, or isobacteriochlorin ring.

The assignment of Ni(I) in reduced nickel F430[10] and isobacteriochlorins[6-8] is unambiguous, but similar definitive conclusions have not been reached for reduced nickel porphyrins, chlorins, or hydroporphyrins. Initial assignments of reduced nickel porphyrins and chlorins as $\pi$-anion radicals were made primarily on the basis of room temperature ESR and UV-visible spectra,[3-5,8] both of which seemed to be definitive. However, more recent results for different Ni(II) porphyrins under different solution conditions indicate that the site of the electroreduction may be all[9] or partially[5,8] at the metal center.

**Scheme I**

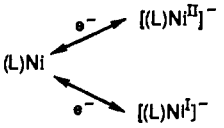


A review of the overall data in the literature seems to suggest that variations in experimental conditions or porphyrin macrocycle can influence the site of electron transfer and/or the electron density on a given singly reduced nickel porphyrin, but little attention has been given to the effect of solvent and the degree of axial ligation. This is discussed in the present paper for two Ni(II) porphyrins which are quite similar in structure, yet have very different half-wave potentials for formation of the singly reduced complex. The structures of these compounds are schematically shown in Figure 1 where ($T(p\text{-}Et_2N)PP$) and ($T(p\text{-}Me_2N)F_4PP$) are the dianions of *meso*-tetrakis(*p*-(diethylamino)phenyl)porphyrin and *meso*-tetrakis(*o,o,m,m*-tetrafluoro-*p*-(dimethylamino)phenyl)porphyrin, respectively.

The two complexes were reduced by controlled potential electrolysis and the resulting products characterized by ESR and thin-layer UV-visible spectroscopy under different solution conditions. Reactions between singly reduced $[(P)Ni]^-$ and $CH_3I$ were also investigated in order to better understand relationships that might exist between thermodynamic potentials, the site of electroreduction, and catalytic reactivity of the reduced complex with alkyl halides.

(1) Kadish, K. M. *Prog. Inorg. Chem.* **1987**, *34*, 435-605.
(2) Kadish, K. M.; Morrison, M. M. *Inorg. Chem.* **1976**, *15*, 980.
(3) Chang, D.; Malinski, T.; Ulman, A.; Kadish, K. M. *Inorg. Chem.* **1984**, *23*, 817.
(4) Kadish, K. M.; Sazou, D.; Liu, Y. M.; Saoiabi, A.; Ferhat, M.; Guilard, R. *Inorg Chem.* **1988**, *27*, 1198.
(5) Kadish, K. M.; Sazou, D.; Maiya, G. B.; Han, B. C.; Liu, Y. M.; Saoiabi, A.; Ferhat, M.; Guilard, R. *Inorg. Chem.* **1989**, *28*, 2542.
(6) Stolzenberg, A. M.; Stershic, M. T. *J. Am. Chem. Soc.* **1988**, *110*, 6391.
(7) Stolzenberg, A. M.; Stershic, M. T. *Inorg. Chem.* **1987**, *26*, 3082.
(8) Renner, M. W.; Forman, A.; Fajer, J.; Simpson, D.; Smith, K. M.; Barkigia, K. M. *Biophys. J.* **1988**, *53*, 277a.
(9) Lexa, D.; Momenteau, M.; Mispelter, J.; Savéant, J.-M.; *Inorg. Chem.* **1989**, *28*, 30.
(10) Jaun, B.; Pfaltz, A. *J. Chem. Soc., Chem. Commun.* **1986**, 1327.

0002-7863/91/1513-512$02.50/0 

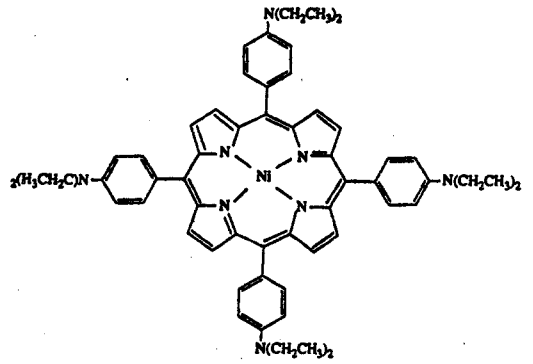


(T(p-$Et_2$N)PP)Ni

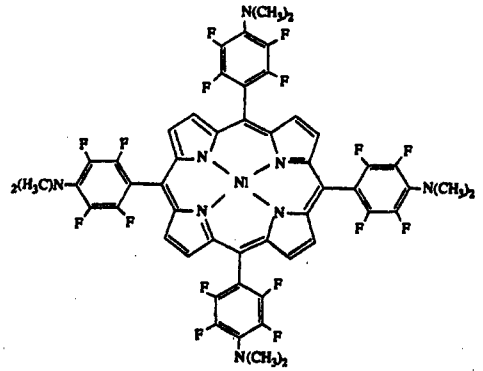


(T(p-$Me_2$N)$F_4$PP)Ni

**Figure 1.** Structures of the investigated porphyrins.

## Experimental Section

**Chemicals.** Tetrahydrofuran (THF), obtained from Mallinckrodt Inc., was distilled over $CaH_2$ and then over sodium benzophenone prior to use. Dimethylformamide (DMF) was purchased from J. T. Baker and was distilled twice under vacuum over 4 Å molecular sieves prior to use. Pyridine (py) was distilled twice under $N_2$ over $CaH_2$ prior to use. Tetra-*n*-butylammonium perchlorate (TBAP) was purchased from Fluka Chemical G.R. The salt was twice recrystallized from absolute ethyl alcohol and dried in a vacuum oven at 40 °C prior to use. Carbon monoxide was purchased from Big Three Ind. and was of CP grade. Methyl iodide was purchased from Aldrich Chemical Co. and used directly.

(T(*p*-$Et_2$N)PP)Ni was synthesized and purified by the method of Adler.[11] (T(*p*-$Me_2$N)$F_4$PP)Ni was synthesized from ($TF_5PP)H_2$ (where $TF_5PP$ is the dianion of *meso*-tetrakis(pentafluorophenylporphyrin)) and nickel acetate in DMF under reflux conditions. The $^1$H NMR spectrum of the isolated product shows two distinct resonances at 8.79 ppm (8 H) and 3.27 ppm (24 H) which are attributed, respectively to the β-pyrrole hydrogens and the hydrogens of the *p*-$Me_2$N group attached to each of the phenyl substituents. The $^{19}$F NMR spectra of this compound shows two resonances of equal intensity at −140.4 and −152.3 ppm which arise from fluorine atoms at the ortho and meta positions of the four phenyl rings. Mass spectral data for the compound show a parent peak at 1131 which is consistent with the calculated molecular weight of the assigned structure. A more detailed description of the synthesis and additional spectroscopic characterization of (T(*p*-$Me_2$N)$F_4$PP)Ni are given in ref 12.

**Instrumentation and Methods.** Cyclic voltammograms were obtained with an IBM Model EC 225 voltammetric analyzer and an Omnigraphic 2000 *X–Y* recorder using a three-electrode system. The working electrode was a 0.80-mm$^2$ platinum button. A platinum wire served as the counter electrode and a homemade saturated calomel electrode (SCE) was used as the reference electrode which was separated from the bulk solution by a glassy diaphragm connected to a bridge filled with the electrolyte solution. All potentials were measured vs SCE. Controlled potential electrolysis was carried out with an EG&G Princeton Applied Research Model 174A Potentiostat/179 coulometer system which was coupled with an EG&G Princeton Applied Research Model RE-0074 time-based *X–Y* recorder. All electrochemical measurements were carried out at 22 ± 1 °C unless otherwise specified.

Thin-layer spectroelectrochemical measurements were taken with a Tracor Northern 6500 multichannel analyzer/controller using an optically transparent platinum gauze working electrode. UV–visible spectra of the neutral complexes were also recorded on an IBM 9430 spectrophotometer.

ESR spectra were taken with a Bruker Model ER 100D spectrometer equipped with an ER 040-X microwave bridge and an ER 080 power supply. The cavity was cooled for low-temperature measurements by a stream of liquid nitrogen that was passed through a variable-temperature insert. The *g* values were measured relative to diphenylpicrylhydrazide (DPPH) ($g$ = 2.0037 ± 0.0002).[13]

$^1$H NMR spectra were recorded on a QE-300 FT NMR spectrometer with $CDCl_3$ as solvent. Chemical shifts were referenced against tetramethylsilane (TMS).

Mass spectra were obtained from a high-resolution hybrid tandem VG Analytical Model 70-SEQ (EEQQ geometry) mass spectrometer. A standard fast atom bombardment (FAB) source was used and *m*-nitrobenzyl alcohol (NBA) was the liquid matrix.

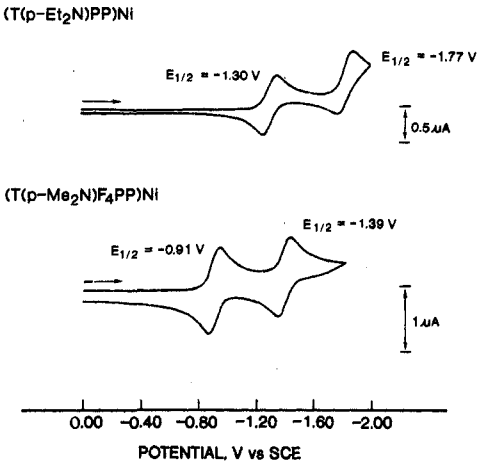


**Figure 2.** Cyclic voltammograms of (a) (T(*p*-$Et_2$N)PP)Ni and (b) (T(*p*-$Me_2$N)$F_4$PP)Ni in THF, 0.1 M TBAP at 23 °C at $v$ = 100 mV/s.

**Table I.** Half-Wave Potentials (V vs SCE) for Electroreduction of (P)Ni in THF, DMF, or py Containing 0.1 M TBAP

| porphyrin | solvent | 1st reduction | 2nd reduction | $\Delta E_{1/2}$,[b] V |
|---|---|---|---|---|
| (T(*p*-$Et_2$N)PP)Ni | THF | −1.30 | −1.77 | 0.47 |
| | DMF[a] | −1.32 | | |
| | py | −1.30 | −1.81 | 0.51 |
| (T(*p*-$Me_2$N)$F_4$PP)Ni | THF | −0.91 | −1.39 | 0.48 |
| | DMF | −0.89 | −1.46 | 0.57 |
| | py | −1.08 | −1.43 | 0.35 |

[a] Low solubility. [b] $\Delta E_{1/2}$ = difference between first and second reduction potential.

## Results and Discussion

**Electroreduction of (P)Ni.** Room temperature cyclic voltammograms of (T(*p*-$Et_2$N)PP)Ni and (T(*p*-$Me_2$N)$F_4$PP)Ni in THF containing 0.1 M TBAP are illustrated in Figure 2 and a summary of reduction potentials in THF, DMF, and pyridine is given in Table I. Both Ni(II) complexes are reduced in two reversible one-electron transfer steps. The difference in $E_{1/2}$ between the two reductions ranges between 350 and 570 mV depending upon the solvent and porphyrin macrocycle and may be compared to a 420 ± 50 mV separation generally observed for porphyrin complexes which undergo reduction at the π-ring system to give π-anion radicals and dianions.[1,14] However, as has been shown numerous times, neither values of $E_{1/2}$ nor separations of $\Delta E_{1/2}$ should be used as definitive diagnostic criteria for assigning the

(11) Adler, A. D.; Longo, F. R.; Kampas, F.; Kim, J. *J. Inorg. Nucl. Chem.* **1970**, *32*, 30.
(12) Kadish, K. M.; Araullo-McAdams, C.; Han, B. C.; Franzen, M. M. *J. Am. Chem. Soc.* **1990**, *112*, 8364.
(13) Drago, R. S. *Physical Methods in Chemistry*; W. B. Saunders: Philadelphia, 1977; p 324.
(14) Fuhrhop, J.-H.; Kadish, K. M.; Davis, D. G. *J. Am. Chem. Soc.* **1973**, *95*, 5140.

**Table II.** UV–Visible Data for Neutral and Singly Reduced (P)Ni in THF, DMF, or py

| porphyrin | solvent | λ, nm (ε × $10^{-4}$, $M^{-1}$ $cm^{-1}$) |
|---|---|---|
| (T(*p*-$Et_2$N)PP)Ni | THF | 442 (19.4); 539 (1.8); 582 (1.2) |
| | DMF[a] | 449; 546; 596 |
| | py | 450 (18.0); 544 (1.7); 590 (1.5) |
| [(T(*p*-$Et_2$N)PP)Ni]$^-$ | THF | 437 (15.6); 530 (1.2); 573 (0.4) |
| | DMF[a] | 441; 528; 673; 887 |
| | py | 441 (16.1); 531 (1.6) |
| (T(*p*-$Me_2$N)$F_4$PP)Ni | THF | 412 (20.8); 527 (1.8); 557 (0.9) |
| | DMF | 411 (11.8); 524 (1.3); 555 (0.7) |
| | py | 433 (41.7); 556 (0.2) |
| [(T(*p*-$Me_2$N)$F_4$PP)Ni]$^-$ | THF | 422 (13.3); 615 (1.2); 851 (0.2) |
| | DMF | 420 (8.5); 522 (1.0); 614 (0.9); 858 (0.6) |
| | py | 423 (13.8); 616 (1.6); 845 (0.6) |

[a] Low solubility. Values of ε could not be determined.

site of electroreduction in a given metalloporphyrin.

(T(*p*-$Et_2$N)PP)Ni is more basic than (T(*p*-$Me_2$N)$F_4$PP)Ni and is consequently harder to reduce. However, the absolute potential difference between the first reduction of the two complexes is not constant from solvent to solvent (see Table I) and varies from 0.43 V in DMF ($E_{1/2}$ = −1.32 and −0.89 V) to 0.22 V in pyridine ($E_{1/2}$ = −1.30 and −1.08 V). These differences can be attributed to different degrees of axial coordination in the two complexes and has been reported for other series of metalloporphyrins.[1]

**ESR Characterization of [(P)Ni]$^-$.** ESR spectra of singly reduced [(P)Ni]$^-$ in THF under three different experimental conditions are illustrated in Figure 3. Figures 3a and 3b show the spectra obtained at room and low temperature under $N_2$ while Figure 3c shows low-temperature spectra of the two complexes under a CO atmosphere. Both singly reduced species have isotropic ESR spectra at room temperature under $N_2$ with $g_{iso}$ values of 2.01 and $\Delta H_{pp}$ = 10 G (see Figure 3a). These spectra are unambiguously assigned as Ni(II) porphyrin π-anion radicals, consistent with reports in the literature for other singly reduced Ni porphyrins at room temperature.[3,5,8]

[(T(*p*-$Et_2$N)PP)Ni]$^-$ and [(T(*p*-$Me_2$N)$F_4$PP)Ni]$^-$ have anisotropic ESR spectra in THF at low temperature under $N_2$ (Figure 3b) with $g_{\parallel}$ = 1.99 or 1.98 and $g_{\perp}$ = 2.01. $\Delta H_{pp}$ ranges from 8.0 to 11.0 G. Other reduced nickel porphyrins have similar ESR spectra at low temperature in THF,[5,8] as does a reduced nickel tetraaza macrocycle complex in propylene carbonate.[15] These spectra were assigned to a Ni(II) porphyrin π-anion radical with some Ni(I) character,[5,8] or, for the case of the tetraaza macrocycle, to a Ni(I) and Ni(II) π-anion radical hybrid.[15]

The ESR spectra of [(P)Ni]$^-$ in THF change dramatically upon going from a $N_2$ to a CO atmosphere at low temperature. Enhanced anisotropic ESR signals with three *g* tensors occur at $g_1$ = 2.10, $g_2$ = 2.01, and $g_3$ = 1.99 for [(T(*p*-$Et_2$N)PP)Ni]$^-$ or at $g_1$ = 2.16, $g_2$ = 2.06, and $g_3$ = 2.01 for [(T(*p*-$Me_2$N)$F_4$PP)Ni]$^-$ as shown in Figure 3c. There are no reports in the literature for CO binding to neutral, oxidized, or reduced nickel porphyrins, but the spectra in Figure 3c are similar to ESR spectra of five-coordinate CO complexes of non-porphyrin Ni(I) derivatives[15,16] and are consistent with the formation of a five-coordinate [(P)Ni(CO)]$^-$ species as shown in eq 1.

$$(P)Ni^{II} + e^- + CO \leftrightarrow [(P)Ni^{I}(CO)]^- \quad (1)$$

Tetrahydrofuran is a weakly coordinating solvent and the ESR signals of [(P)Ni]$^-$ in THF at room or low temperature (Figures 3a and 4a) are those of a Ni(II) porphyrin π-anion radical or a Ni(II) porphyrin π-anion radical with some Ni(I) character. In contrast, both DMF and py can strongly coordinate to [(P)Ni]$^-$ and this leads to Ni(I) low-temperature ESR spectra for both [(T(*p*-$Et_2$N)PP)Ni]$^-$ and [(T(*p*-$Me_2$N)$F_4$PP)Ni]$^-$. The resulting anisotropic ESR spectra in DMF have g values of 2.10, 2.01, and

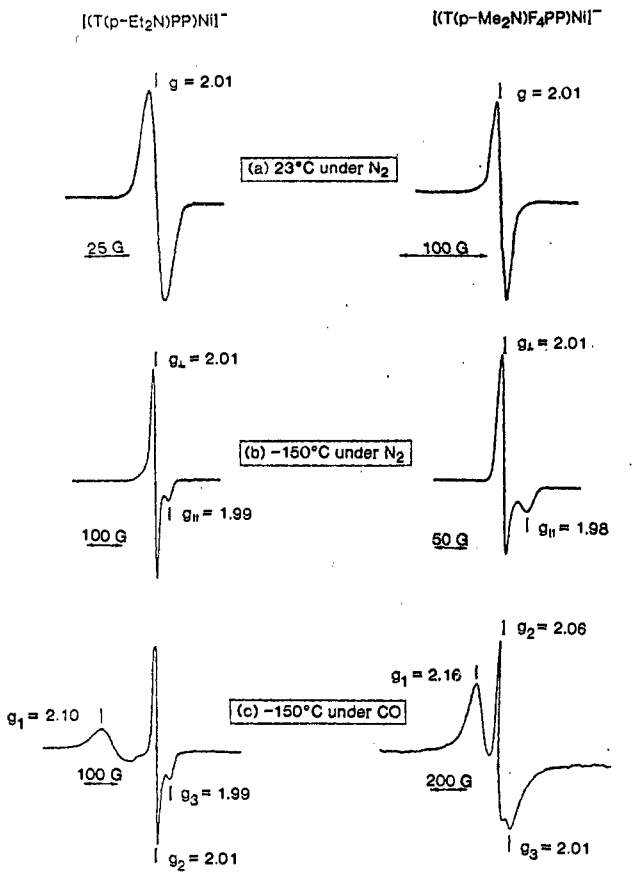


Figure 3. ESR spectra of [(T(*p*-$Et_2$N)PP)Ni]$^-$ and [(T(*p*-$Me_2$N)$F_4$PP)Ni]$^-$ in THF, 0.2 M TBAP, at (a) 23 °C under $N_2$, (b) −150 °C under $N_2$, and (c) −150 °C under CO.

**Scheme II**

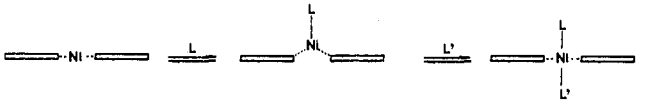


1.93 for [(T(*p*-$Et_2$N)PP)Ni]$^-$ and 2.10, 2.00, and 1.95 for [(T(*p*-$Me_2$N)$F_4$PP)Ni]$^-$. These spectra are illustrated in Figure 4b and are almost identical in shape to the spectra of [(P)$Ni^{I}$(CO)]$^-$ in THF under CO (Figure 3c).

The spectrum of [(T(*p*-$Et_2$N)PP)Ni]$^-$ in pyridine (Figure 4c) is also similar to the one obtained in THF (Figure 4a) and is characterized as a Ni(II) porphyrin π-anion radical with some Ni(I) character. In contrast, Ni(I) is present for [(T(*p*-$Me_2$N)$F_4$PP)Ni]$^-$ in pyridine under $N_2$ (Figure 4c), in DMF under $N_2$ (Figure 4b), or in THF under CO (Figure 3c).

The overall data in Figures 3 and 4 suggest that a Ni(I) complex is formed only under conditions where a five-coordinate species is generated. (P)Ni and [(P)Ni]$^-$ may exist as 5- or 6-coordinated species[17] but the exact coordination number will depend on several factors including the type of substituents on the porphyrin macrocycle.[18] These ligand addition reactions are schematically shown for neutral (P)Ni in Scheme II where L is CO, DMF, or pyridine. Similar ligand binding reactions should also be observed for the singly reduced [(P)Ni]$^-$ derivative.

The nickel ion should be forced out of the porphyrin plane and the ESR spectrum should be anisotropic when [(P)Ni]$^-$ is axially

(15) Gagné, R. R.; Ingle, D. M. *Inorg. Chem.* **1981**, *20*, 420.
(16) Gagné, R. R.; Ingle, D. M. *J. Am. Chem. Soc.* **1980**, *102*, 1444.
(17) (a) Findsen, E. W.; Shelnutt, J. A.; Friedman, J. M.; Ondrias, M. R. *Chem. Phys. Lett.* **1986**, *126*, 465. (b) Pasternack, R. F.; Spiro, E. G.; Teach, M. *J. Inorg. Nucl. Chem.* **1974**, *36*, 599. (c) McLees, B. D.; Caughey, W. S. *Biochemistry* **1968**, *7*, 642. (d) Kirner, J. F.; Garofalo, J., Jr.; Scheidt, W. R. *Inorg. Nucl Chem. Lett.* **1975**, *11*, 107. (e) Cole, S. J.; Curthoys, G. C.; Magnusson, E. A.; Phillips, J. N. *Inorg. Chem.* **1972**, *11*, 1024.
(18) Walker, F. A.; Hui, E.; Walker, J. M. *J. Am. Chem. Soc.* **1975**, *97*, 2390.

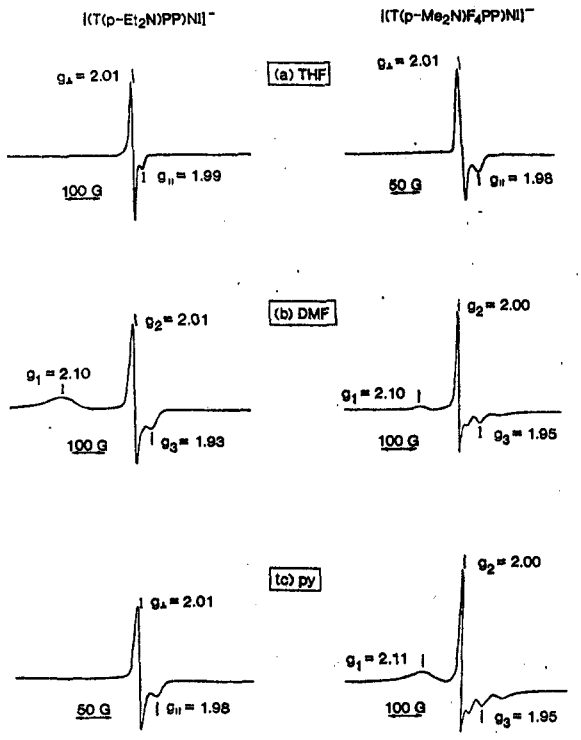


**Figure 4.** ESR spectra of $[(T(p\text{-}Et_2N)PP)Ni]^-$ and $[(T(p\text{-}Me_2N)F_4PP)Ni]^-$ at −150 °C in (a) THF, (b) DMF, and (c) py containing 0.2 M TBAP.

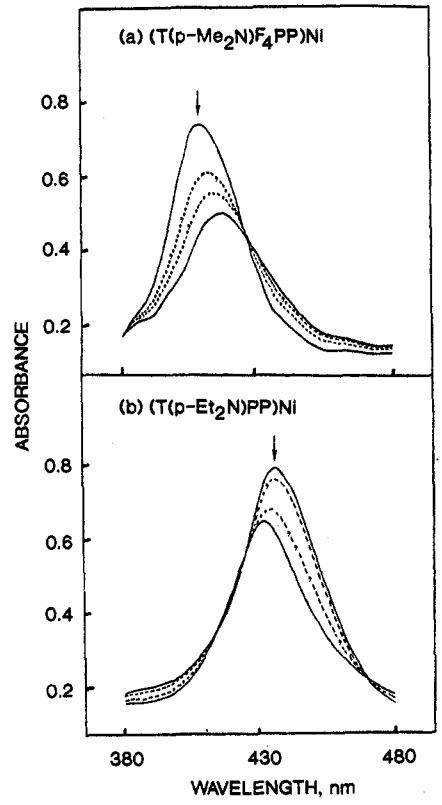


**Figure 5.** Thin-layer spectral changes obtained upon eletroreduction of (a) $(T(p\text{-}Me_2N)F_4PP)Ni$ at $E = -1.10$ V and (b) $(T(p\text{-}Et_2N)PP)Ni$ at $E = -1.45$ in THF, 0.2 M TBAP.

coordinated by a single ligand (such as in DMF for P = $T(p\text{-}Et_2N)PP$ and $T(p\text{-}Me_2N)F_4PP$ or in pyridine for P = $T(p\text{-}Me_2N)F_4PP$). However, the nickel ion of six-coordinate $[(P)Ni(L)_2]^-$ should be more in the plane of the porphyrin ring and might therefore be predicted to have an ESR spectrum similar to that of the four-coordinate species. This is indeed the case as shown for $[(T(p\text{-}Et_2N)PP)Ni]^-$ which has almost the same spectrum in pyridine and THF (see Figures 4a and 4c).

**UV–Visible Characterization of $[(P)Ni]^-$.** The different basicities of the $T(p\text{-}Et_2N)PP$ and $T(p\text{-}Me_2N)F_4PP$ macrocycles are not reflected in the room or low temperature ESR spectra of $[(P)Ni]^-$ in THF (see Figure 3) but differences clearly exist in the UV–visible spectroelectrochemistry of the two complexes.

The Soret and visible bands of $(T(p\text{-}Me_2N)F_4PP)Ni$ are red shifted upon reduction and there is a significant drop in the bands' molar absorptivity (Figure 5a). In contrast, the Soret and visible bands of $(T(p\text{-}Et_2N)PP)Ni$ undergo a blue shift upon electroreduction (Figure 5b) and there are only small changes in the molar absorptivity of the absorption bands. A broad band appears between 600 and 700 nm after the addition of one electron to $(T(p\text{-}Me_2N)F_4PP)Ni$ and this suggest that the first reduction of the complex is porphyrin ring-centered at room temperature.[19] A broad band in this region is also observed upon formation of $[(T(p\text{-}Et_2N)PPNi]^-$, but this band is of weaker intensity than that for $[(T(p\text{-}Me_2N)F_4PP)Ni]^-$, indicating less $\pi$-anion radical character for the electrogenerated species.

The type of spectral changes upon reduction of $(T(p\text{-}Et_2N)PP)Ni$ have been observed when genuine Ni(I) complexes are generated from Ni(II) derivatives such as $(OEiBC)Ni$[6,7] and, in the present case, suggest that the electroreduction of $(T(p\text{-}Et_2N)PP)Ni$ is all, or partially, at the nickel center. The reduction of both (P)Ni complexes is electrochemically and spectrally reversible in a thin-layer cell and the initial UV–visible spectrum of $(P)Ni$[11] could be quantitatively recovered upon controlled potential reoxidation of the reduced species at 0.00 V.

A coordination of DMF or py to the metalloporphyrin complex should induce red shifts in the UV–visible absorption bands, with the shifts being greater for the Soret band than the Q bands.[20] The absorption peaks are red shifted for $[(T(p\text{-}Et_2N)PP)Ni]^-$ in DMF or py, compared to the spectrum of the same species in THF (see Table II), and this would indicate that the reduced complex is ligated. The exact coordination number is unknown, but the ESR spectra for $[(T(p\text{-}Et_2N)PPNi]^-$ in Figure 4 were interpreted as being due to a five-coordinate species in DMF and a six-coordinate species in py. The UV–visible data provide no spectral evidence for DMF ligation to singly reduced $[(T(p\text{-}Me_2N)F_4PP)Ni]^-$, but some interaction must exist since a Ni(I) ESR spectrum is obtained.

**Reactions of $[(P)Ni]^-$ with Methyl Iodide.** Figure 6 illustrates cyclic voltammograms of $(T(p\text{-}Et_2N)PP)Ni$ and $(T(p\text{-}Me_2N)F_4PP)Ni$ in THF with and without added $CH_3I$. The first reduction of both porphyrin complexes is reversible in THF alone and occurs at $E_{1/2} = -1.30$ V for $(T(p\text{-}Et_2N)PP)Ni$ or −0.91 V for $(T(p\text{-}Me_2N)F_4PP)Ni$. The addition of 7–8 equiv of $CH_3I$ to these solutions results in an irreversible reduction of $(T(p\text{-}Et_2N)PP)Ni$ (Figure 6b) but only slightly affects the reduction of $(T(p\text{-}Me_2N)F_4PP)Ni$ (Figure 6c).

The cathodic peak for reduction of $(T(p\text{-}Et_2N)PP)Ni$ is located at $E_p = -1.40$ V in THF containing 7.1 equiv of $CH_3I$ and the peak current is enhanced by a factor of about 3.8 compared to reduction of the same complex in THF alone (see Figure 6b). The reduction of $(T(p\text{-}Me_2N)F_4PP)Ni$ remains reversible to quasi-reversible in solutions containing low concentrations of $CH_3I$ but becomes irreversible in THF containing greater than 100 equiv of $CH_3I$. This is illustrated in Figure 6c for a THF solution containing 183.7 equiv of $CH_3I$. Under these conditions, the cathodic peak current is enhanced by a factor of 1.8 compared to the reduction of $(T(p\text{-}Me_2N)F_4PP)Ni$ in THF alone. This suggests an overall reduction by two electrons. Also, an anodic peak appears at $E_p = 0.30$ V after scanning past potentials corresponding to the first reduction of both (P)Ni complexes, and this peak is attributed to an oxidation of free $I^-$. The direct

(19) Gouterman, M. In *The Porphyrins*; Dolphin, D., Ed.; Academic: New York, 1979; Vol. III, pp 17–18.

(20) Corwin, A. H.; Chivvis, A. B.; Poor, R. W.; Whitten, D. G.; Baker, E. W. *J. Am. Chem. Soc.* **1968**, *90*, 6577.

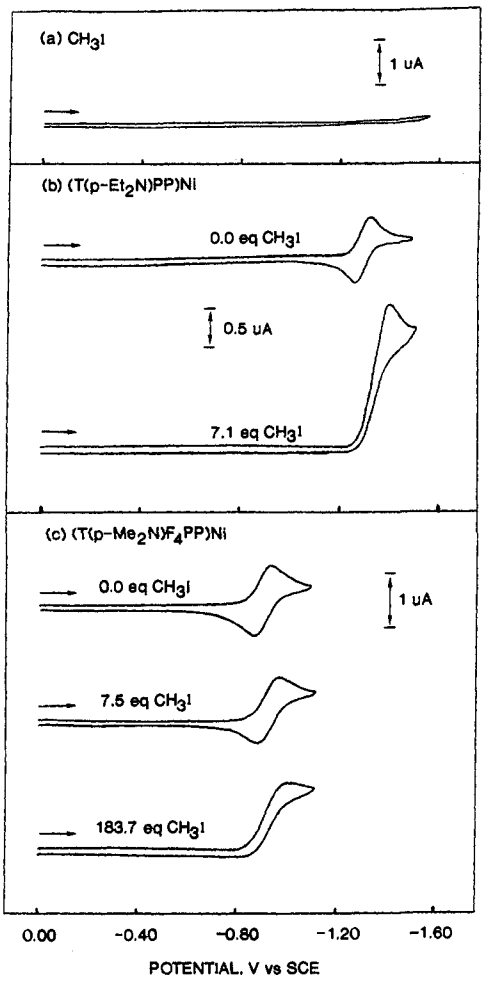


**Figure 6.** Cyclic voltammograms of (a) $3.0 \times 10^{-3}$ M $CH_3I$, (b) $4.4 \times 10^{-4}$ M (T(*p*-$Et_2N$)PP)Ni and (c) $1.4 \times 10^{-3}$ M (T(*p*-$Me_2N$)$F_4$PP)Ni in THF, 0.1 M TBAP, with various concentrations of $CH_3I$ at $v = 100$ mV/s.

**Scheme III**

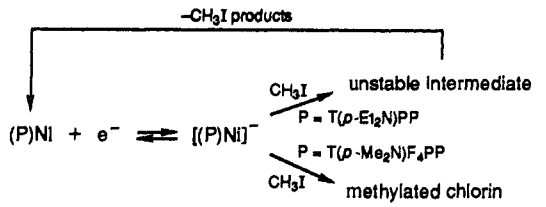


reduction of $CH_3I$ does not occur in THF up to potentials of −1.60 V, and this is shown by the cyclic voltammogram in Figure 6a. Under these conditions, an oxidation peak for free $I^-$ is also not observed.

The UV–visible and ESR data indicate a different degree of Ni(I) character in the two singly reduced $[(P)Ni]^-$ complexes and this is also reflected in the reactivity of these species with $CH_3I$ in THF. Two different products are formed and the overall reactions involve a branching scheme of the type illustrated in Scheme III.

The degree of Ni(I) character in the reactive species is related to the ability of $[(P)Ni]^-$ to catalytically reduce low concentrations of $CH_3I$. There are increased catalytic currents for reduction of $[(T(p\text{-}Et_2N)PP)Ni]^-$ in THF containing $CH_3I$, and the diagnostic plot in Figure 7 indicates that this species has more Ni(I) character than $[(T(p\text{-}Me_2N)F_4PP)Ni]^-$. This assignment is consistent with the spectral and spectroelectrochemical results previously described.

Several mechanisms might be proposed to explain the electrocatalytic activity of $[T(p\text{-}Et_2N)PP)Ni]^-$, but the most probable involves a conversion of $(P)Ni^{II}$ to $[(P)Ni^{I}]^-$ which then reacts

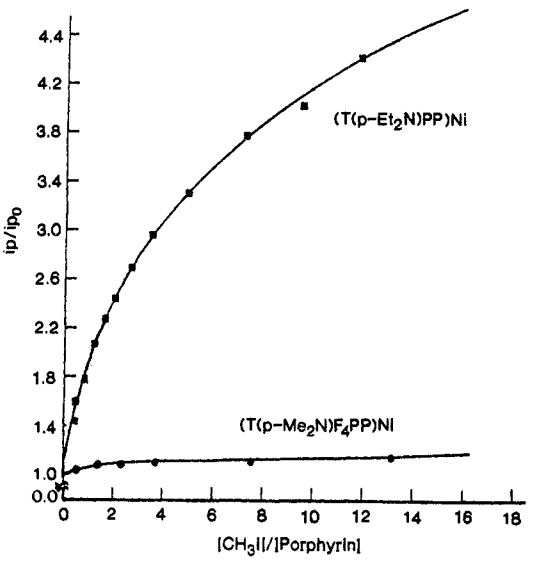


**Figure 7.** Plot of $ip/ip_0$ vs $[CH_3I]/[(P)Ni]$ ratio were ip and $ip_0$ are the measured cathodic peak currents for the first reduction of (P)Ni in the presence and absence of $CH_3I$, respectively.

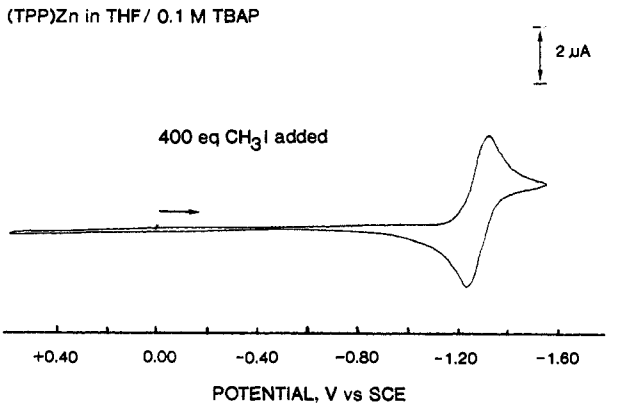


**Figure 8.** Cyclic voltammogram of $5.0 \times 10^{-4}$ M (TPP)Zn in THF, 0.1 M TBAP, after the addition of 400 equiv of $CH_3I$ at $v = 100$ mV/s.

with $CH_3I$ to form an unstable $\sigma$-bonded product which decomposes to regenerate the initial Ni(II) species. The reduction of (OEiBC)Ni leads to a definitive Ni(I) complex which, in the presence of alkyl halides,[21] is also thought to proceed by a similar mechanism. However, (OEiBC)Ni($CH_3$) has never been isolated. The isolation of (T(*p*-$Et_2N$)PP)Ni($CH_3$) was also not possible, and only the original Ni(II) species was recovered after purification of the product resulting from a mixture of electrogenerated $[(T(p\text{-}Et_2N)PP)Ni]^-$ and excess $CH_3I$ under $N_2$ in the absence of an applied potential.

The catalytic reduction of $CH_3I$ by (T(*p*-$Et_2N$)PP)Ni might also involve an outer-sphere mechanism in which $[(P)Ni]^-$ reacts with $CH_3I$ to generate the initial Ni(II) porphyrin which is further reduced at this potential. This type of mechanism should be independent of the porphyrin central metal ion and dependent only on the half-wave potential for formation of $[(P)M]^-$ from (P)M. If this mechanism were operative, (TPP)Zn, which has a similar half-wave potential ($E_{1/2} = -1.33$ V) to that of (T(*p*-$Et_2N$)PP)Ni, should react with $CH_3I$ in a catalytic fashion. This is not the case. Even in the presence of 400 equiv of $CH_3I$, there is no apparent reaction between reduced (TPP)Zn and $CH_3I$. Under these solutions conditions, the first reduction remains completely reversible (see Figure 8) which clearly indicates the absence of an outer-sphere mechanism in the observed catalytic reduction of $CH_3I$ by $[(T(p\text{-}Et_2N)PP)Ni]^-$. The data also indicate that a low valent

(21) Stolzenberg, A. M.; Stershic, M. T. *J. Am. Chem. Soc.* **1988**, *110*, 5397.

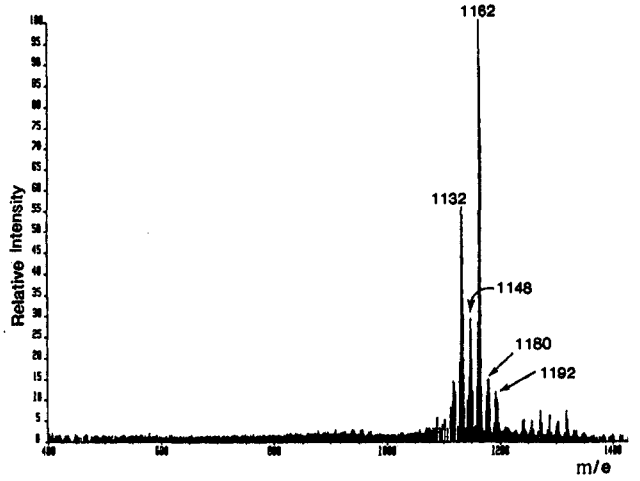


**Figure 9.** Mass spectrum of product obtained after mixing electrogenerated [(T(*p*-$Me_2N$)$F_4$PP)Ni]$^-$ with excess $CH_3I$ in THF under $N_2$ in the absence of an applied potential.

metal center is needed in order for the singly reduced species to catalytically react with $CH_3I$.

Singly reduced [(T(*p*-$Me_2N$)$F_4$PP)Ni]$^-$ also reacts with $CH_3I$ but this reaction is not catalytic. The product isolated after mixing electrogenerated [(T(*p*-$Me_2N$)$F_4$PP)Ni]$^-$ with excess $CH_3I$ under $N_2$ in the absence of an applied potential is not the initial (T(*p*-$Me_2N$)$F_4$PP)Ni complex, but rather a $\beta$-pyrrole methylated nickel chlorin. A mass spectrum of the isolated reduction product is shown in Figure 9 and has peaks consistent with species containing one, two, three, or four $CH_3$ groups at the $\beta$-pyrrole positions of the (T(*p*-$Me_2N$)$F_4$PP)Ni macrocycle. These peaks are located at 1148, 1162, 1180, and 1192 amu, respectively. The most intense peak at 1162 amu corresponds to a species that has two $CH_3$ attached groups while the 1132 amu peak corresponds to unmethylated (T(*p*-$Me_2N$)$F_4$PP)Ni (MW = 1130.2).

The UV–visible spectrum of the reduction product shows an intense absorption at 620 nm which is characteristic of a chlorin-type species.[3,22] $^1$H NMR resonances of this product[23] are similar to resonances of known methylated nickel chlorins[22,24] and suggest that the major product generated from [(T(*p*-$Me_2N$)$F_4$PP)Ni]$^-$ and $CH_3I$ has the structure illustrated below:

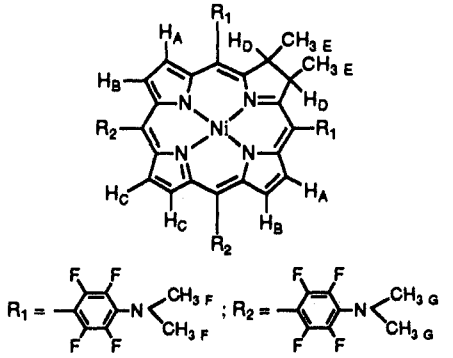


The formation of a $\beta$-pyrrole methylated chlorin as a stable reaction product is consistent with a high electron density on the porphyrin ring and has also been observed to occur upon addition of $CH_3I$ to singly reduced (TPP)Ru(CO)[25] as well as to doubly reduced (OEP)Ni.[26] This type of reaction does not occur for [(T(*p*-$Et_2N$)PP)Ni]$^-$ which catalytically reduces $CH_3I$ and this would seem to imply that there is less electron density on the conjugated $\pi$-ring system of this species. In this regard, it should be noted that despite the similar basicities of OEP and T(*p*-$Et_2N$)PP, the reductive methylation of (OEP)Ni[26] occurs after a two-electron chemical reduction of the porphyrin to give [(OEP)Ni]$^{2-}$. This type of reaction apparently does not occur for electroreduced [(OEP)Ni]$^-$ which is reported to catalytically reduce alkyl halides.[21]

In summary, the results in this paper clearly demonstrate that temperature, type of porphyrin macrocycle, solvent, and axial ligand coordination will all influence the electroreduction site in (P)Ni and can lead to the formation of Ni(I) porphyrins, Ni(II) porphyrin $\pi$-anion radicals, or Ni(II) porphyrin $\pi$-anion radicals with some Ni(I) character. The electrogenerated [(P)Ni]$^-$ species give different products upon reaction with $CH_3I$ in THF and this is also indicative of different Ni(I) character in each of the singly reduced [(P)Ni]$^-$ complexes.

**Acknowledgment.** The support of the National Institutes of Health (Grant GM-25172) and the National Science Foundation (Grant CHE-8822881) is gratefully appreciated. We also appreciate several useful discussions with Dr. Jack Fajer.

(22) Ulman, A.; Fisher, D.; Ibers, J. A. *J. Heterocycl. Chem.* **1982**, *19*, 409.

(23) $^1$H NMR $\delta$ values (in ppm) for the product formed in the reaction between [(T(*p*-$Me_2N$)$F_4$PP)Ni]$^-$ and $CH_3I$ in THF: $H_A$ 8.00 (d); $H_B$ 8.45 (d); $H_C$ 8.35 (s); $H_D$ 3.74 (q); $CH_{3E}$ 0.98 (d); $CH_{3F}$ 2.67 (s); $CH_{3G}$ 2.69 (s).

(24) Scheer, H.; Katz, J. J. In *Porphyrins and Metalloporphyrins*; Smith, K. M., Ed.; Elsevier: New York, 1975; pp 440–4.

(25) Kadish, K. M.; Deng, Y. Unpublished results.

(26) Dwyer, P. N.; Buchler, J. W.; Scheidt, W. R. *J. Am. Chem. Soc.* **1974**, *96*, 2789.